Cell Reports
Medicine

Article

Increased intestinal bile acid absorption contributes to age-related cognitive impairment

Graphical abstract

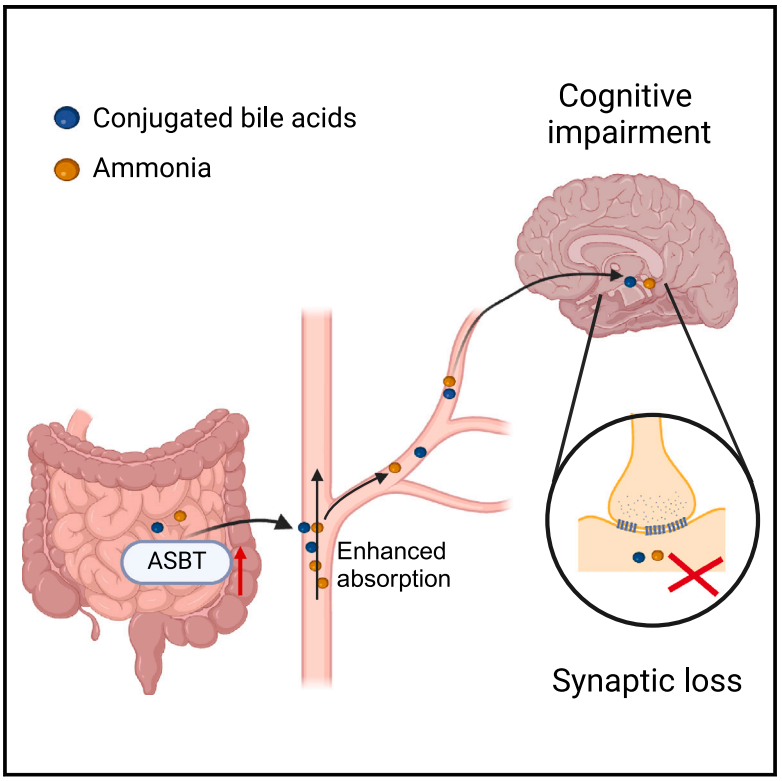

Authors

Zhenxing Ren, Ling Zhao, Mingliang Zhao, ..., Yajun Tang, Guoxiang Xie, Wei Jia

Correspondence

weijia2@hku.hk

In brief

Ren et al. uncover that enhanced gut absorption of conjugated primary bile acids (CPBAs) and ammonia accelerates cognitive decline with age, which a bile acid sequestrant, cholestyramine, can counter. This study connects bile acid metabolism with cognitive aging and suggests a possible pathway for intervention.

Highlights

- Age-related cognitive decline linked to CPBAs and ammonia levels
- Brain CPBAs and ammonia drive synapse loss
- ASBT boosts CPBA and ammonia intake in gut
- Cholestyramine reduces CPBA absorption, improving cognitive impairment

Ren et al., 2024, Cell Reports Medicine *5*, 101543
May 21, 2024
https://doi.org/10.1016/j.xcrm.2024.101543

CellPress

Cell Reports Medicine

CellPress
OPEN ACCESS

Article

Increased intestinal bile acid absorption contributes to age-related cognitive impairment

Zhenxing Ren,[1,7] Ling Zhao,[2,7] Mingliang Zhao,[1] Tianhao Bao,[3] Tianlu Chen,[1] Aihua Zhao,[1] Xiaojiao Zheng,[1] Xinru Gu,[1] Tao Sun,[1] Yuhuai Guo,[4] Yajun Tang,[1] Guoxiang Xie,[5] and Wei Jia[1,6,8,*]

[1]Center for Translational Medicine and Shanghai Key Laboratory of Diabetes Mellitus, Shanghai Sixth People's Hospital Affiliated with Shanghai Jiaotong University School of Medicine, Shanghai 200233, China
[2]School of Integrative Medicine, Shanghai University of Traditional Chinese Medicine, Shanghai 201203, China
[3]The Affiliated Mental Health Center of Kunming Medical University, Kunming, Yunnan 650224, China
[4]School of Kinesiology, Shanghai University of Sport, Shanghai 200438, China
[5]Human Metabolomics Institute, Inc., Shenzhen, Guangdong 518109, China
[6]Department of Pharmacology and Pharmacy, University of Hong Kong, Hong Kong, China
[7]These authors contributed equally
[8]Lead contact
*Correspondence: weijia2@hku.hk
https://doi.org/10.1016/j.xcrm.2024.101543

SUMMARY

Cognitive impairment in the elderly is associated with alterations in bile acid (BA) metabolism. In this study, we observe elevated levels of serum conjugated primary bile acids (CPBAs) and ammonia in elderly individuals, mild cognitive impairment, Alzheimer's disease, and aging rodents, with a more pronounced change in females. These changes are correlated with increased expression of the ileal apical sodium-bile acid transporter (ASBT), hippocampal synapse loss, and elevated brain CPBA and ammonia levels in rodents. *In vitro* experiments confirm that a CPBA, taurocholic acid, and ammonia induced synaptic loss. Manipulating intestinal BA transport using ASBT activators or inhibitors demonstrates the impact on brain CPBA and ammonia levels as well as cognitive decline in rodents. Additionally, administration of an intestinal BA sequestrant, cholestyramine, alleviates cognitive impairment, normalizing CPBAs and ammonia in aging mice. These findings highlight the potential of targeting intestinal BA absorption as a therapeutic strategy for age-related cognitive impairment.

INTRODUCTION

The aging population, especially females, is susceptible to the development of cognitive impairment, a risk factor for neurodegenerative diseases such as Alzheimer's disease (AD).[1] In these individuals, impaired cognitive function manifests through pathological phenotypes, including β-amyloid (Aβ) deposition, formation of neurofibrillary tangles, neuronal loss, synaptic defects, and neurotrophic failure.[2,3] Despite these well-defined characteristics, the precise pathogenic mechanism underlying aging-related cognitive impairment remains uncertain.

Recent studies have suggested a link between changes in bile acids (BAs) and age-related cognitive impairment.[4–6] Investigations into AD and Parkinson's disease reveal that lower serum levels of unconjugated primary BAs (UPBAs), such as cholic acid and chenodeoxycholic acid, along with elevated levels of glycochenodeoxycholic acid, a conjugated primary BA metabolite, are closely associated with the severity of cognitive decline symptoms.[7–9] Current understanding suggests that the gut microbiota, which produces secondary BAs in the gastrointestinal lumen, undergoes age-related alterations. These changes significantly impact the levels of BAs circulating in the body and present within the brain.[10] Additionally, there is a notable correlation between certain serum BA metabolites, particularly increased levels of glycolithocholic acid and tauro-lithocholic acid, which are bacterially derived secondary BAs, and elevated (CSF) total tau levels.[9] BAs can communicate between the periphery and the brain either through specific BA transporters or by passive diffusion across the blood-brain barrier.[11]

Despite the widespread expression of BA receptors in neurons and glial cells, certain BAs, such as ursodeoxycholic acid and tauroursodeoxycholic acid, exhibit neuroprotective properties by attenuating neuroinflammation, apoptosis, or endoplasmic reticulum stress.[12–14] Conversely, the accumulation of cytotoxic BAs, such as deoxycholic acid and lithocholic acid, is known to damage cell membranes, promote the production of reactive oxygen species, and induce endoplasmic reticulum stress, which can lead to mitochondrial dysfunction. These processes can ultimately lead to the apoptosis or necrosis of liver cells.[15] Despite these insights, the ways in which the BA profile alters with aging, and whether these alterations play a role in cognitive decline, are still not fully understood.

In our prior studies, we demonstrated that enhanced intestinal absorption of conjugated BAs via apical sodium-BA

transporter (ASBT), leading to elevated ammonia levels, exacerbates neurotoxic effects in human patients and rodents experiencing liver failure.[16] Conjugated BAs, especially taurine conjugates, possess high solubility and play a crucial role in maintaining the acidic pH balance of the intestinal lumen.[17,18] The disruption of this balance, resulting from increased active intestinal absorption, may contribute to the excessive generation of neurotoxic ammonia in an elevated-pH luminal environment.[19] Building upon our prior findings, this study aimed to elucidate a BA-driven pathogenic mechanism underlying age-related cognitive impairment.

RESULTS

An increase in circulating CPBAs and ammonia is associated with age-related cognitive decline in humans and rodents

In a healthy population (cohort I) ranging from 20 to 80 years old (n = 682), a significant decline in serum total BAs levels was found within the subgroup aged 60 to 80 compared to the two younger subgroups (20–39 and 40–59; Figure 1A). This decrease in the elderly individuals was mainly attributed to reduced levels of UPBAs and unconjugated secondary BAs (USBAs; Figure 1B). Unexpectedly, we observed an increase in the proportion of CPBAs among the elderly participants (Figure 1B). This increase was significant in females aged 60–80 years, as shown in Figure 1C, where the mean percentage of CPBAs was markedly higher. The relative levels of CPBAs showed a positive correlation with age in both genders (Figure 1D).

In another cohort (cohort II), consisting of individuals with mild cognitive impairment (MCI), both genders of patients (n = 243) exhibited increased percentages of serum CPBAs compared to age-matched controls (n = 292). The percentage of serum CPBAs demonstrated a negative correlation with cognitive scores, with a more pronounced relationship observed in females (Figures 1E and 1F). Serum ammonia levels were significantly elevated in both genders of MCI patients and displayed a reverse correlation with the cognitive status of patients (Figures 1G and 1H).

Additionally, analysis of cohort III (N= 637) from the Alzheimer's Disease Neuroimaging Initiative (ADNI) database (http://adni.loni.usc.edu/) revealed that females with MCI who progressed to AD exhibited a higher proportion of CPBAs in their total serum BAs compared to those whose MCI did not progress (Figure 1I). In male patients, there was a minor increase in CPBA percentage, but this did not reach statistical significance. These findings from human subjects suggest a strong link between elevated levels of circulating CPBAs and ammonia with the development of cognitive impairment, with this association appearing more pronounced in females.

To further investigate these findings, we compared serum BAs, ammonia, and cognitive performance between young (24-week-old) and elderly (111-week-old) rodents of both genders. The data revealed that aged rats and mice exhibited lower levels of total serum BAs compared to their corresponding young counterparts (Figures S1A and S1E). Additionally, a decrease in gene expression of hepatic BA synthetase cholesterol 7 alpha-hydroxylase (CYP7A1) was observed in both genders of aged rodents (Figures S1B and S1F), suggesting a decline in hepatic BA biosynthesis with age.

Notably, aged rodents showed significant increases in the proportions of CPBAs in serum total BAs and serum ammonia levels. This was accompanied by a decline in cognitive performance. Particularly, in both young (24 weeks) and old (111 weeks) rodents, there were no significant differences in the levels of serum CPBAs, ammonia, and behaviors between males and females (Figures 1J–1O, S1C, and S1G). These rodent data support the human findings, indicating an association between elevated circulating CPBAs and ammonia levels with age-related cognitive impairment.

Excess levels of CPBAs and ammonia contribute to hippocampal synapse loss

There was no significant difference in the mean of brain total BAs in rats or mice (Figures S2A and S2C), and an increase in circulating CPBAs and ammonia in aged rodents led to elevated levels of these metabolites in the brain, showing no gender-specific changes when compared to young controls (Figures 2A, 2B, 2I, and 2J). Notably, the brains of aged rodents exhibited a higher abundance of CPBAs, particularly taurocholic acid (TCA) (Figures 2C, 2D, 2K, and 2L). The comprehensive BA profile, detailed with concentration or percentage data, also showed a significant increase in TCA levels in elderly rodents (Figures S2E–S2H). Considering that the brain has the function to mediate BA metabolism,[11] we further assessed the expression of *Cyp27a1* and *Cyp46a1*, known as key enzymes in the brain's alternative BA metabolic pathways. We observed a reduction in *Cyp27a1* gene expression in aged rodents, with no differences between genders, whereas *Cyp46a1* expression significantly increased in aged female rodents (Figures S2B and S2D). Concurrent with declined cognitive performance, hippocampal synapse loss was clearly observed in both genders of aged rodents relative to young controls (Figures 2E, 2F, 2M, and 2N). The protein levels of synapsin I (Syn1), a reliable marker of presynaptic vesicles,[20] were decreased in the hippocampus of aged rodents in both genders and showed negative correlations with the proportion of brain TCA and brain ammonia levels (Figures 2G, 2H, 2O, and 2P). These animal data suggest a reverse association between hippocampal synapse loss and excess levels of brain CPBAs and ammonia.

We further investigated the effect of TCA and ammonia on primary neurons of the fetal rat hippocampus and synaptic function. After 24 h of incubation with TCA or ammonia, TCA (25 and 50 μM) and ammonia (2.5 and 5 mM) individually decreased the levels of gene and protein expression of the synaptic markers Syn1 and postsynaptic density protein 95 (Psd95) (Figures S3A and S3B). Immunofluorescence data using labeling for Syn1 (pre-synapses marked by green puncta) and Psd95 (post-synapses marked by red puncta) revealed that 50 μM TCA or 5 mM ammonia significantly reduced the numbers of co-localized puncta in neurons compared to the vehicle group (Figures S3C and S3D). Moreover, when compared to individual TCA or ammonia interventions, the combination of 25 μM TCA and 2.5 mM ammonia significantly inhibited synaptic protein expressions and decreased the number of colocalized puncta. These

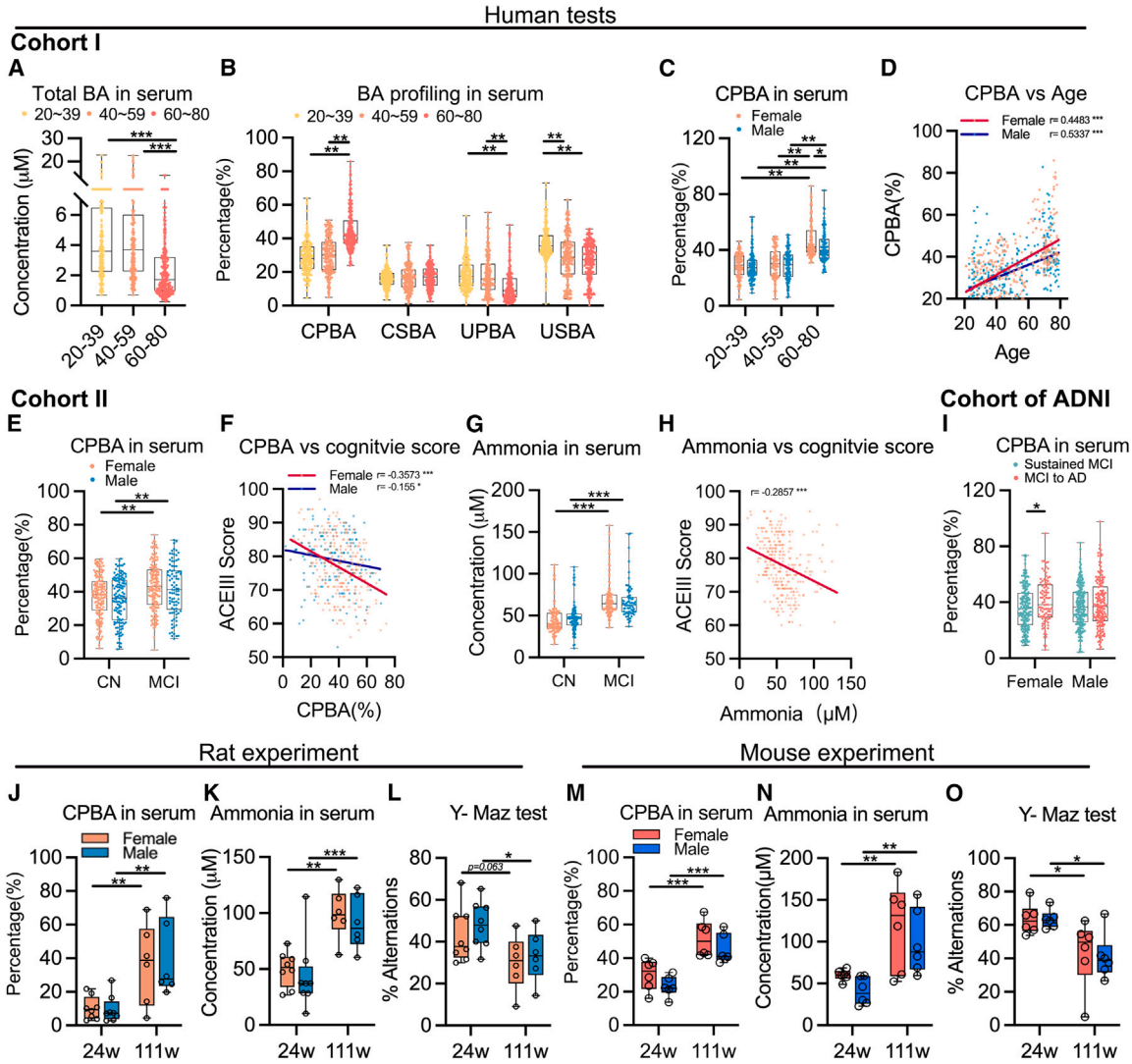

Figure 1. The increase of conjugated primary BAs and ammonia in the serum is associated with age-related cognitive decline in human beings and rodents

(A) The concentrations of serum total BAs in a healthy population (N = 682 in the cohort I) aged from 20 to 80.

(B) The percentages of conjugated primary BAs (CPBAs), conjugated secondary BAs (CSBAs), unconjugated primary BAs (UPBAs), and unconjugated secondary BAs (USBAs) among total serum BAs.

(C) The proportion of serum CPBA among the three age subgroups in both genders.

(D) The relationship between the proportion of serum CPBA and age in the healthy cohort resulted from Pearson r correlation analysis (females highlighted in red; males highlighted in blue).

(E) The proportion of serum CPBA in both genders of healthy controls and patients with mild cognitive impairment (MCI) from cohort II (N = 535).

(F) The correlation between serum percentages of CPBA and cognitive score evaluated with ACEIII (Addenbrooke's cognitive examination) in females (red) and males (blue).

(G and H) The serum ammonia level of samples (N = 379) from cohort II and the correlation between ammonia concentration and ACEIII score (N = 280).

(I) The proportion of serum CPBA in both genders of MCI patients (N = 637) resulted from the ADNI database (http://adni.loni.usc.edu/) with a follow-up monitoring of disease progression. $^{*}p < 0.05$; p values were from logic regression models adjusting age, gender, BMI, education year, and APOE-4.

(J and M) The percentages of CPBA in serum total BAs in both genders of rodents (n = ~6–8/group).

(K and N) the concentration of serum ammonia in both genders of rodents (n = ~6–8/group).

(L and O) The cognitive performance data in both genders of rodents resulted from the Y-maze test (n = ~6–8/group).

The comparison of serum total BA levels among groups was analyzed with one-way ANOVA, and comparisons of CPBA, ammonia and behavior data in either human beings or rodents were performed with two-way ANOVA. The statistical difference is labeled as follows: $^{*}p < 0.05$, $^{**}p < 0.01$, $^{***}p < 0.001$. See also Figure S1 and Tables 1 and 2.

Table 1. The baseline information of cohort II from C-PAS (Chinese Preclinical Alzheimer's Disease Study)

Cohort II	All (n = 535)	CN (n = 292)	MCI (n = 243)
Age (years)	65.26 ± 8.17	64.18 ± 8.28	66.56 ± 7.86
Sex (M/F)	218/317	128/164	90/153
BM-FIXED	23.5 ± 4.01	23.63 ± 3.82	23.34 ± 4.23
Education-FIXED (years)	11.84 ± 2.99	12.37 ± 2.99	11.21 ± 2.86
ACEIII score	77.63 ± 8.42	82.17 ± 6.32	72.35 ± 7.43

Data are presented as mean ± SEM values.

Table 2. The baseline information of cohort III from ADNI

Cohort III	All (n = 637)	Sustained MCI (n = 390)	MCI to AD (n = 247)
Age (years)	72.54 ± 7.48	71.79 ± 7.65	73.7 ± 7.06
Sex (M/F)	368/269	211/179	157/90
BM-FIXED	26.96 ± 4.75	27.39 ± 4.87	26.29 ± 4.48
Education-FIXED (years)	16 ± 2.79	16.06 ± 2.81	15.91 ± 2.75
ADAS-13 score	16.52 ± 6.78	13.95 ± 5.89	20.61 ± 6.07

Data are presented as mean ± SEM.

findings suggest that TCA and ammonia, individually and synergistically, can cause hippocampal synaptic loss.

Enhanced intestinal BA absorption and intraluminal ammonia in aging rodents

As part of the enterohepatic circulation process, BAs are synthesized and conjugated in the liver, actively absorbed from the distal ileum into the portal vein, and subsequently returned to the liver. The increased proportion of CPBAs in elderly rodents suggests an enhanced level of intestinal absorption, as the impact of hepatic BA synthesis can be excluded based on the reduced expression of *Cyp7a1*. We examined the expression of these BA transporters in 24-week-old and 111-week-old rodents. The results showed that ASBT was highly expressed in the ileum of aged rodents at both the gene and protein levels, with more pronounced changes observed in females (Figures 3A, 3B, 3I, and 3J). Additionally, the gene expression of *Ostβ* and *Mrp3* was enhanced in aged females, while *Mrp2* was decreased with age in females, and *Ostα* showed no significant difference among the groups (Figures 3C–3F and 3K–3N). Consistent with the changes in BA transporters, CPBAs exhibited reduced amounts in the ileal contents of aged female rodents (Figures S1D and S1H). These findings indicate an enhanced active absorption of BAs in the intestine of aging rodents, particularly in females.

Subsequently, we measured the pH and ammonia levels, which revealed higher levels of intraluminal pH and ammonia in aged rodents, particularly in females (Figures 3G, 3H, 3O, and 3P). These results indicate an enhanced active absorption of BAs in the intestine of aging rodents, leading to the overproduction of luminal ammonia, especially in females.

ASBT-dependent intestinal BA absorption modulates cognitive performance and influences the levels of peripheral and central CPBAs and ammonia in rodents

The upregulation of ileal *Sgk1* (serum/glucocorticoid regulated kinase 1), the target gene of the glucocorticoid receptor (GR), in aging rodents, especially in females, supports the enhanced intestinal BA active absorption with age in a gender-specific manner (Figures S4A and S4F).

To investigate the causal role of intestinal BA active absorption in regulating CPBAs, ammonia, and cognitive performance, we manipulated the intestinal transport capability in rats and mice of both genders using a GR agonist, dexamethasone (DEX; 1 mg/kg for 2 weeks), and an ASBT inhibitor, GSK2330672 (GSK; 1 mg/kg for 2 weeks) (Figure 4A). In rats, DEX significantly decreased the cumulative duration with no significant change in total distance in the open field test and reduced the percentage of alterations in the Y-maze test, indicating impaired cognition (Figures 4B, 4C, and S4B). However, these cognitive deficits were reversed when DEX was co-administered with GSK. DEX treatment elevated the protein level of ileal ASBT in rodents, with more pronounced changes in females (Figure 4D). While DEX increased serum total BAs in rats without affecting the levels in the ileal contents and brain (Figures S4C and S4D), GSK was able to counteract the DEX-induced elevation of serum total BAs while significantly increasing ileal total BAs. There was no difference in total BAs in the rat hippocampus among the groups (Figure S4E). The proportions of CPBAs in total BAs increased in the serum and brain of DEX-treated rats but decreased in the ileal contents (Figures 4E and 4F). Consistent with these changes, serum and brain ammonia levels were elevated in DEX-treated rats but remained similar to control levels in rats treated with the combination of GSK and DEX (Figures 4G and 4H). Similar alterations in cognitive performance, total BAs, CPBAs, and ammonia levels were observed in mice following DEX intervention alone or in combination with GSK (Figures 4I–4M and S4F–S4I).

Cholestyramine attenuates intestinal BA absorption and alleviates cognitive impairment in aged mice

We administered a chow diet containing 2% cholestyramine (CLS) to 111-week-old male mice for 3 months (Figure 5A). Elderly mice exhibited impaired cognitive performance, as evidenced by a reduced cumulative duration in the open field test and a decreased percentage of alterations in the Y-maze test. However, feeding these aged mice with CLS significantly improved this abnormal cognitive performance (Figures 5B and 5C).

Total BA levels in the ileal contents and feces showed no significant differences between young and old mice but exhibited a substantial increase in CLS-fed aged mice (Figures S5A and S5B). While there was a slight downregulation of total BAs in the serum of aged mice, no differences were observed in the brain (Figures S5C and S5D). CLS had no impact on the levels of total BAs in the serum or brain but significantly enhanced the proportion of CPBAs in the ileal contents of aging mice (Figure 5D). Conversely, it attenuated the proportions of CPBAs in the brain, although it had no effect on means of serum CPBA percentage (Figures 5E and 5F). The elevated levels of ammonia in the serum and brain of aging mice returned to normal levels upon CLS intervention (Figures 5G and 5H). These findings

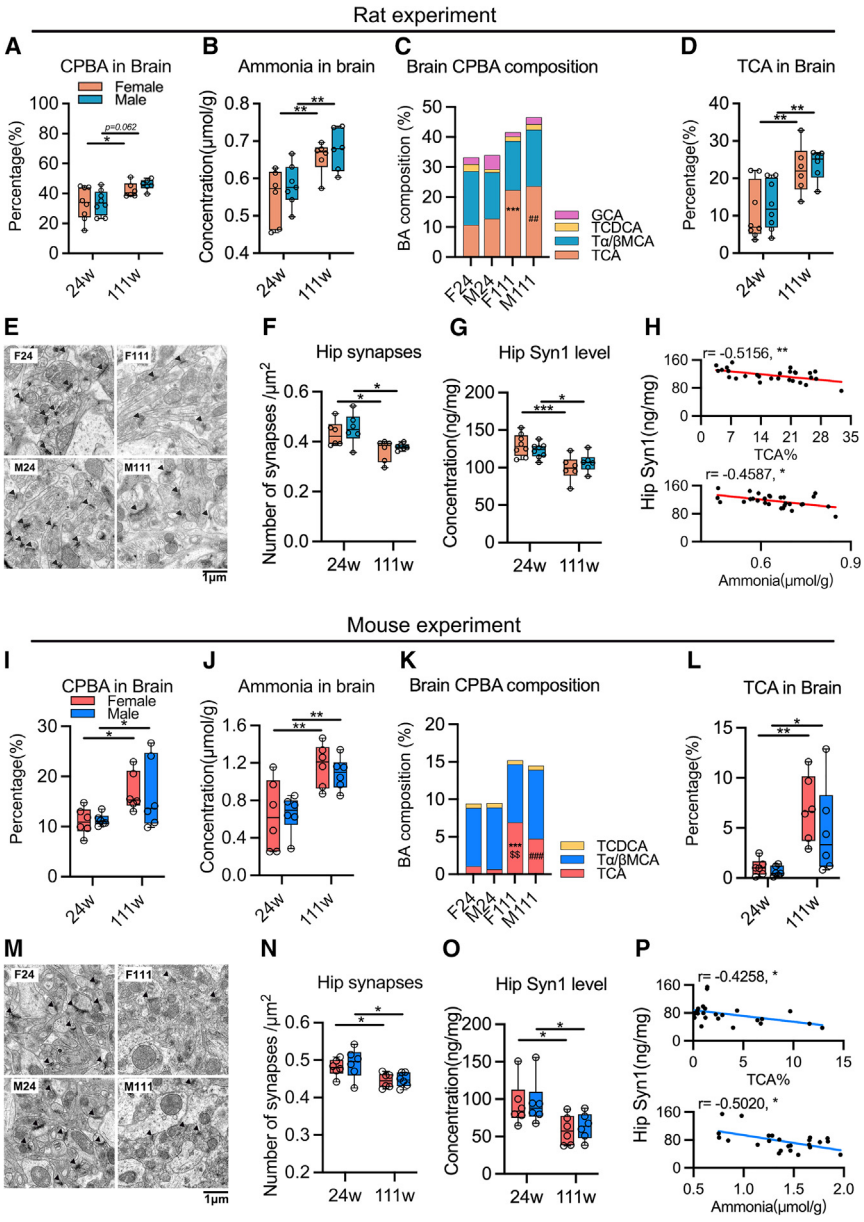

Figure 2. The excess of CPBA and ammonia in the brain is associated with hippocampal synapse loss in aging rodents

(A–D and I–L) The percentages of CPBAs and ammonia level as well as the CPBA composition (e.g., taurocholic acid [TCA]) in the brain of rodents in both genders (n = ∼6–8/group).

(E, F, M, and N) The representative images and counts of hippocampal synapses in rats and mice resulted from transmission electron microscopy (n = ∼6–8/group, 3 repeats/sample).

(G and O) The concentrations of hippocampal Synapsin 1 (Syn1) in both genders of rodents (n = 6∼8/group, 3 repeats/sample).

(H and P) Pearson's r correlation between hippocampal Syn1 level and brain TCA or ammonia in rodents.

The comparisons of CPBA, ammonia, and synapse data in rodents were performed with two-way ANOVA. The statistical difference is labeled as follows: ***p < 0.005 vs. 24-week female (F24); ##p < 0.01; ###p < 0.005 vs. 24-week male (M24); $$$p$ < 0.01 vs. 111-week male (M111) for the comparison of the CBPA composition among groups; *p < 0.05; **p < 0.01; ***p < 0.001 for other comparisons. See also Figures S2 and S3.

suggest that attenuation of intestinal BA absorption by CLS can improve cognitive decline and alleviate the excess of CPBAs and ammonia in aging mice.

DISCUSSION

This study demonstrates that enhanced intestinal BA absorption via ASBT contributes to age-related cognitive impairment. Increased levels of CPBAs, such as TCA, and ammonia accumulate in the brain due to enhanced intestinal BA absorption, leading to hippocampal synapse loss. These findings propose a new hypothesis linking BA metabolism to age-related cognitive decline and provide a proof-of-concept strategy for mitigating cognitive impairment.

Peripheral changes in BA levels with aging have been reported. Fasting plasma BA levels decrease in older men, while long-lived mice exhibit increased serum, liver, and bile BA levels.[21,22] Clinical studies also indicate decreased liver expression of *CYP7A1* and reduced postprandial serum BA levels in older individuals.[23,24] These observations suggest a reduced peripheral BA pool due to decreased BA synthesis in the elderly.

Consistent with this, our study supports lower BA synthesis in aged rodents. Total serum BA levels decrease, accompanied by downregulated hepatic *Cyp7a1* expression. Our previous work has thoroughly investigated both the classic and alternative BA synthesis pathways, focusing on key hepatic enzymes such as *Cyp7a1*, *Cyp27a1*, *Cyp8b1*, and *Cyp7b1*. Notably, all of these enzymes demonstrate reduced activity with aging.[25] This evidence suggests that hepatic BA synthesis does not primarily drive the elevated levels of CPBAs, such as TCA, in the circulation and brains of aging rodents. Additionally, we explored the roles of two crucial brain-derived regulators of BA synthesis, *Cyp27a1* and *Cyp46a1*.[11] We observed upregulated expression of *Cyp46a1* but downregulated expression of *Cyp27a1* in the hippocampus of aged rodents. Similar changes in CYP46A1 and CYP27A1 have been reported in the brains of AD patients.[26] This suggests a potential influence of brain-specific molecular factors on the BA profile changes associated with aging.

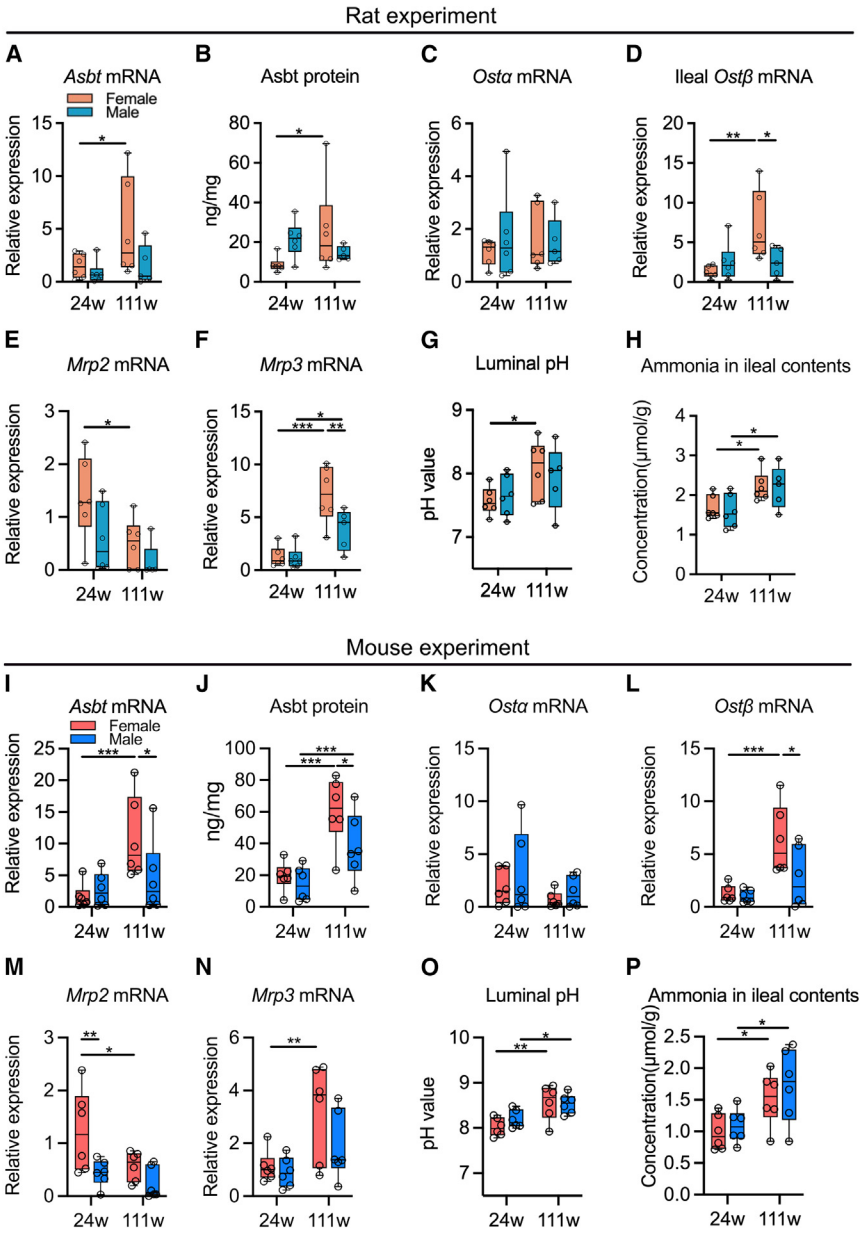

Figure 3. The declined cognitive performance and hippocampal synapse loss are associated with the levels of brain TCA and ammonia

(A and B) Intestinal Asbt gene and protein expression of rats (n = ~5–6/group, 3 repeats/sample).

(C–F) The mRNA expression of BA transport-related genes, including ileal *Mrp2*, *Mrp3*, *Ostα*, and *Ostβ* in rat ileum (n = ~5–6/group, 3 repeats/sample).

(G) The pH value of luminal contents in rats.

(H) The ammonia level in ileal contents of rats.

(I and J) Intestinal Asbt gene and protein expression of mice (n = 6/group, 3 repeats/sample).

(K–N) The mRNA expression of BA transport-related genes, including ileal *Mrp2*, *Mrp3*, *Ostα*, and *Ostβ* in mouse ileum (n = 6/group, 3 repeats/sample).

(O) The pH value of luminal contents in mice.

(P) The ammonia level in ileal contents of mice.

Two-way ANOVA analyzed the statistics, and the significance is expressed as follows: $^{*}p < 0.05$, $^{**}p < 0.01$, $^{***}p < 0.001$ vs. the 24-week group. See also Figure S1 and Table S1.

Conversely, intestinal BA absorption increases with age, as evidenced by elevated ileal ASBT expression and serum CPBA levels. Although some studies suggest decreased active absorption of TCA in the ileum of aged male mice,[27] *in vivo* evidence supports increased intestinal BA active transport with age, including higher levels of taurine-conjugated primary BAs in the circulation and bile of aged mice.[25,28] Enhanced intestinal BA absorption is more pronounced in aging females, likely influenced by hormonal fluctuations during peri- and postmenopausal periods, including increased glucocorticoids that transactivate ASBT.[29] Besides enhanced BA active transport, we cannot rule out another possible mechanism whereby the aged gut microbiota, showing a major shift with a reduced bacterial diversity and decreased bile salt hydrolase activity,[30,31] might contribute to increased CPBA levels in serum in both humans and rodents.

BAs, particularly those with strong acidity, regulate intraluminal pH, which controls ammonium-ammonia conversion. In an alkaline environment, intraluminal ammonium converts to ammonia, freely diffusing into the blood.[32] Manipulating ASBT activity reveals that enhanced intestinal BA absorption leads to excess ammonia levels in the serum and brain. Neurotoxic ammonia accumulation promotes neurological pathophysiology, including memory loss, through synaptic dysfunction and neurotransmitter imbalances.[33] Given the predominance of gram-negative bacteria in the gut microbiota of the elderly,[34] which are known to express the ammonia synthetase urease,[35] we speculate that the aged gut microbiota constitutes another significant source of excess ammonia.

Elderly rodents exhibit cognitive decline and increased hippocampal synapse loss, further supporting the connection between enhanced intestinal BA and ammonia absorption and cognitive impairment. Clinical studies also associate increased ileal BA-binding protein levels with AD and MCI[16] and elevated circulating CPBAs with cognitive decline in diabetes and cirrhosis patients.[16,36]

We demonstrate that TCA induces synapse loss, suggesting its pathogenic role in cognitive decline. Central BAs, including TCA, have been associated with cognitive function in postmortem brain samples.[37] The exact mechanisms underlying BA-mediated cognitive impairment require further investigation.

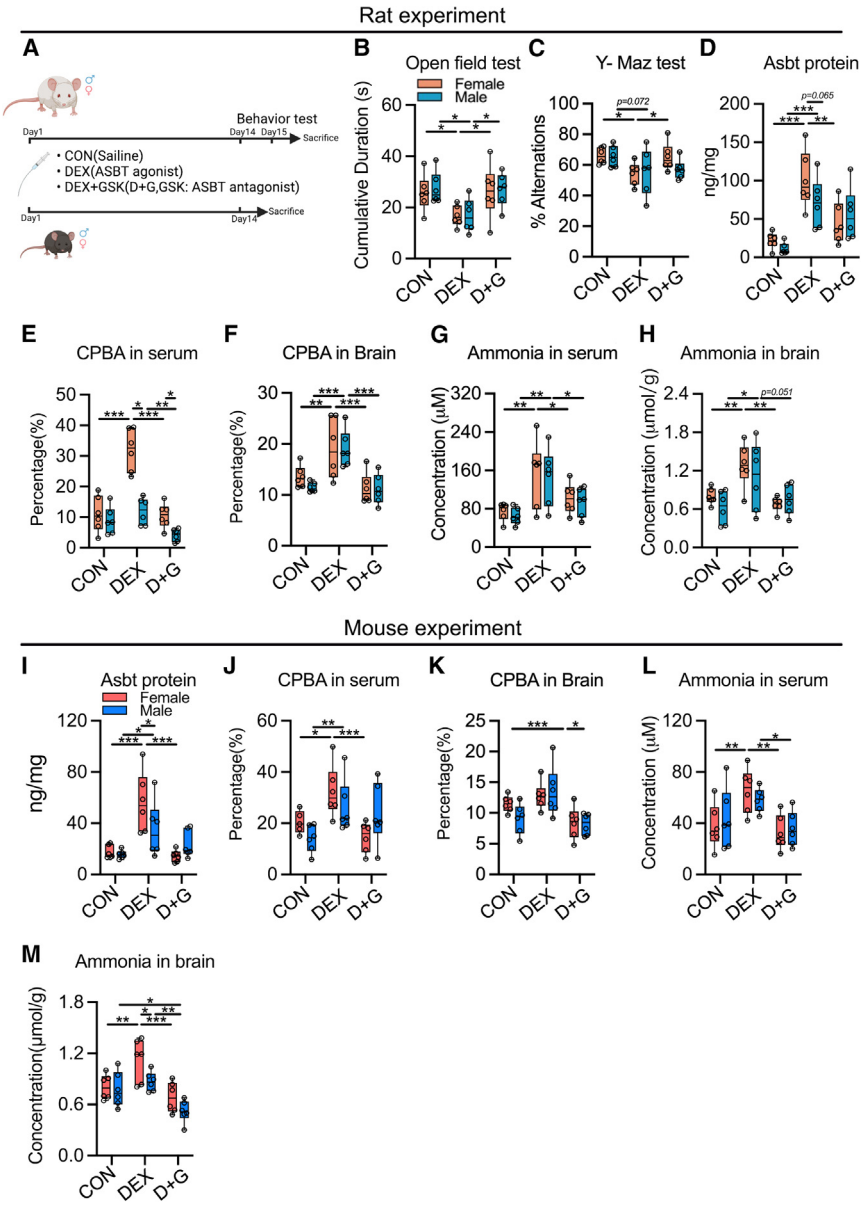

Figure 4. The impacts of the Asbt activator and inhibitor on the cognitive performance and levels of brain CPBAs and ammonia in rodents

(A) An overview of the animal experiment of Asbt manipulation.

(B and C) Open field test and Y-maze spontaneous alteration test (n = 6/group).

(D) The rats' ileal Asbt protein level tested by ELISA (n = 6/group, 3 repeats/sample).

(E and F) The CPBA percentage of rat serum and brain tissue (n = 6/group).

(G and H) The serum and brain ammonia levels in rats (n = 6/group, 3 repeats/sample).

(I) The mice's ileal Asbt protein level tested by ELISA (n = 6/group, 3 repeats/sample).

(J and K) The CPBA percentage of mouse serum and brain tissue (n = 6/group).

(L and M) The serum and brain ammonia levels in mice (n = 6/group, 3 repeats/sample).

Two-way ANOVA analyzed the statistics, and the significance is expressed as follows: $^{*}p < 0.05$, $^{**}p < 0.01$, $^{***}p < 0.001$. See also Figure S4 and Table S1.

TCA receptors, such as farnesoid X receptor and Takeda G protein-coupled receptor 5, expressed in neuronal and glial cells,[38,39] play contributive roles in the modulation of amino acid catabolism, ammonium detoxification, and synaptic function.[40,41] We suppose that the mechanism by which TCA induces synapse loss and, thus, cognitive function may involve the activation of BA signaling.

Previous research on hepatic encephalopathy highlights the detrimental effects of enhanced ASBT expression and abnormal conjugated BA and ammonia absorption on cognition.[16] Our study demonstrates that upregulating ASBT expression with DEX treatment induces cognitive decline, while concurrent administration of GSK, an ASBT inhibitor, rescues cognitive deficits and reduces BA and ammonia overabsorption. It's important to note that targeting ASBT impacts not just BA levels but also other factors associated with cognitive impairment. Previous studies uncovered that inhibiting ASBT leads to decreased levels of low-density lipoprotein cholesterol[42,43] and reduced glucose levels, which, in turn, prevents a decrease in insulin levels.[44] Both hypercholesterolemia and hyperglycemia are considered risk factors for cognitive decline, while enhancing insulin sensitivity in the brain is recognized as a key strategy for protecting against or treating cognitive impairment.[45] Therefore, we believe that ASBT may mediate additional mechanisms beyond the BA-related actions we explored.

We used a BA-binding resin, CLS, for the treatment of cognitive impairment in this study, which showed improved cognition in elderly mice with significantly reduced brain CPBA percentage while kept in serum. Regarding reduced levels of CPBA in the brain after CLS administration, we suspect that it results from reduced brain permeability of serum BAs. CLS has been reported to significantly reduce circulating toxic molecules like lipopolysaccharides,[46] which could alleviate the increased permeability of the aged blood-brain barrier.[47] We also speculate that increased BA synthesis in the liver would impact the BA enterohepatic circulation but not significantly impact serum BA levels. Although an increased amount of BAs discharged into the intestine could potentially be reabsorbed into the blood, CLS also significantly increased the expression of sodium/taurocholate co-transporting polypeptide in mouse livers,[48] enhancing the reuptake of CPBA from the blood into the liver. As a result, CPBA levels in the blood did not exhibit a significant change.

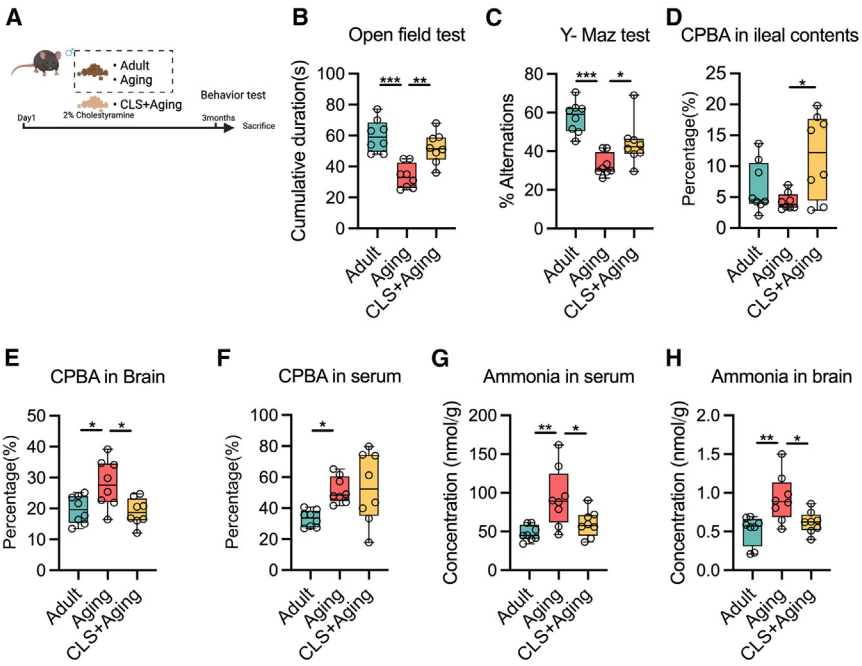

Figure 5. The cognitive performance and the levels of CPBAs and ammonia in serum and brain of aged mice fed with normal or CLS-containing chow

(A) An overview for CLS-treated mice.

(B and C) Open field test and Y-maze spontaneous alteration test (n = 8/group).

(D–F) The ileal content, brain, and serum CPBA percentages in mice (n = 8/group).

(G and H) The serum and brain ammonia in mice (n = 8/group, 3 repeats/sample).

Two-way ANOVA analyzed the statistics, and the significance is expressed as follows: $^{*}p < 0.05$, $^{**}p < 0.01$, $^{***}p < 0.001$. See also Figure S5.

Our study carries significant translational implications. The distinct patterns of BAs and ammonia in serum and/or brain underscore their potential as biomarkers for developing diagnostic methods for AD or age-associated cognitive decline. Moreover, our findings highlight the role of gut ASBT-mediated BA transport as a promising therapeutic target against cognitive deterioration linked to aging. This supports the notion of a gut-brain axis-based intervention as a viable strategy for addressing AD and age-related cognitive challenges.

Limitations of the study

Our study has certain limitations that merit consideration. First, we did not account for the potential impact of an aging gut microbiome, which might elevate CPBA levels due to decreased bile salt hydrolase activity in both humans and rodents. Second, targeting the ASBT affects not just BA levels but also cholesterol and glucose levels, which could also influence cognitive function. This suggests that ASBT's role might extend beyond BA-related mechanisms. Furthermore, the exact mechanism through which TCA leads to synaptic loss needs clearer definition. Future research should delve into these areas for an improved understanding of BA metabolism's role in cognitive health.

STAR★METHODS

Detailed methods are provided in the online version of this paper and include the following:

SUPPLEMENTAL INFORMATION

Supplemental information can be found online at https://doi.org/10.1016/j.xcrm.2024.101543.

ACKNOWLEDGMENTS

This work was supported by the National Key R&D Program of China (2021YFA1301300) and National Natural Science Foundation of China (81974073). We appreciate ADNI for providing the data used in cohort III. Data collection and sharing for ADNI cohorts was funded by the Alzheimer's Disease Neuroimaging Initiative (ADNI) (National Institutes of Health grant U01 AG024904) and DOD ADNI (Department of Defense award W81XWH-12-2-0012). ADNI is funded by the National Institute on Aging, the National Institute of Biomedical Imaging and Bioengineering, and through generous contributions from the following: AbbVie; Alzheimer's Association; Alzheimer's Drug Discovery Foundation; Araclon Biotech; BioClinica, Inc.; Biogen; Bristol-Myers Squibb Company; CereSpir, Inc.; Eisai Inc.; Elan Pharmaceuticals, Inc.; Eli Lilly and Company; EuroImmun; F. Hoffmann-La Roche Ltd. and its

affiliated company Genentech, Inc.; Fujirebio; GE Healthcare; IXICO Ltd.; Janssen Alzheimer Immunotherapy Research & Development, LLC.; Johnson & Johnson Pharmaceutical Research & Development LLC.; Lumosity; Lundbeck; Merck & Co., Inc.; Meso Scale Diagnostics, LLC.; NeuroRx Research; Neurotrack Technologies; Novartis Pharmaceuticals Corporation; Pfizer Inc.; Piramal Imaging; Servier; Takeda Pharmaceutical Company; and Transition Therapeutics. The Canadian Institutes of Health Research is providing funds to support ADNI clinical sites in Canada. Private sector contributions are facilitated by the Foundation for the National Institutes of Health (www.fnih.org). The grantee organization is the Northern California Institute for Research and Education, and the study is coordinated by the Alzheimer's Disease Cooperative Study at the University of California, San Diego. Data used in preparation of this article were obtained from the ADNI database (adni.loni.usc.edu). As such, the investigators within the ADNI contributed to the design and implementation of ADNI and/or provided data but did not participate in analyses or writing of this report. A complete listing of ADNI investigators can be found at http://adni.loni.usc.edu/wp-content/uploads/how_to_apply/ADNI_Acknowledgement_ List.pdf. The metabolomics data of the ADNI cohort were provided by the Alzheimer's Disease Metabolomics Consortium (ADMC). As such, the investigators within the ADMC, not listed specifically in this publication's author's list, provided data along with their pre-processing and prepared them for analyses but did not participate in analyses or writing of this manuscript. A complete listing of ADMC investigators can be found at https://sites.duke.edu/adnimetab/team/.

AUTHOR CONTRIBUTIONS

W.J. was the principal investigator of this study and conceptualized the study. Z.R. and L.Z. conducted critical experiments and drafted the manuscript. M.Z., Y.G., and Y.T. conducted the animal experiments and culture of rat primary hippocampal neurons. X.Z. and X.G. experimented with ~24- to 111-week-old rats. A.Z. and G.X. performed metabolomics profiling of bile acids. T.B., T.C., and T.S. provided data analyses. Z.R., L.Z., and W.J. critically revised the manuscript.

DECLARATION OF INTERESTS

The authors declare no competing interests.

Received: August 14, 2023
Revised: December 27, 2023
Accepted: April 9, 2024
Published: May 1, 2024

REFERENCES

1. Lin, S., and Chen, M. (2022). Gender-specific impact of cognitive impairment on all-cause mortality in older persons: A meta-analysis. Exp. Gerontol. *165*, 111860. https://doi.org/10.1016/j.exger.2022.111860.
2. Bussian, T.J., Aziz, A., Meyer, C.F., Swenson, B.L., van Deursen, J.M., and Baker, D.J. (2018). Clearance of senescent glial cells prevents tau-dependent pathology and cognitive decline. Nature *562*, 578–582. https://doi.org/10.1038/s41586-018-0543-y.
3. Koss, D.J., Jones, G., Cranston, A., Gardner, H., Kanaan, N.M., and Platt, B. (2016). Soluble pre-fibrillar tau and β-amyloid species emerge in early human Alzheimer's disease and track disease progression and cognitive decline. Acta Neuropathol. *132*, 875–895. https://doi.org/10.1007/s00401-016-1632-3.
4. Bonfili, L., Cuccioloni, M., Gong, C., Cecarini, V., Spina, M., Zheng, Y., Angeletti, M., and Eleuteri, A.M. (2022). Gut microbiota modulation in Alzheimer's disease: Focus on lipid metabolism. Clin. Nutr. *41*, 698–708. https://doi.org/10.1016/j.clnu.2022.01.025.
5. Li, T., Yang, S., Liu, X., Li, Y., Gu, Z., and Jiang, Z. (2023). Dietary neoagarotetraose extends lifespan and impedes brain aging in mice via regulation of microbiota-gut-brain axis. J. Adv. Res. *52*, 119–134. https://doi.org/10.1016/j.jare.2023.04.014.
6. Shao, Y., Ouyang, Y., Li, T., Liu, X., Xu, X., Li, S., Xu, G., and Le, W. (2020). Alteration of Metabolic Profile and Potential Biomarkers in the Plasma of Alzheimer's Disease. Aging Dis. *11*, 1459–1470. https://doi.org/10.14336/AD.2020.0217.
7. MahmoudianDehkordi, S., Arnold, M., Nho, K., Ahmad, S., Jia, W., Xie, G., Louie, G., Kueider-Paisley, A., Moseley, M.A., Thompson, J.W., et al. (2019). Altered Bile Acid Profile Associates with Cognitive Impairment in Alzheimer's Disease – An Emerging Role for Gut Microbiome. Alzheimers Dement. *15*, 76–92. https://doi.org/10.1016/j.jalz.2018.07.217.
8. Chen, M.-K., Mecca, A.P., Naganawa, M., Finnema, S.J., Toyonaga, T., Lin, S.-F., Najafzadeh, S., Ropchan, J., Lu, Y., McDonald, J.W., et al. (2018). Assessing Synaptic Density in Alzheimer Disease With Synaptic Vesicle Glycoprotein 2A Positron Emission Tomographic Imaging. JAMA Neurol. *75*, 1215–1224. https://doi.org/10.1001/jamaneurol.2018.1836.
9. Nho, K., Kueider-Paisley, A., MahmoudianDehkordi, S., Arnold, M., Risacher, S.L., Louie, G., Blach, C., Baillie, R., Han, X., Kastenmüller, G., et al. (2019). Altered bile acid profile in mild cognitive impairment and Alzheimer's disease: Relationship to neuroimaging and CSF biomarkers. Alzheimers Dement. *15*, 232–244. https://doi.org/10.1016/j.jalz.2018.08.012.
10. Boehme, M., Guzzetta, K.E., Wasén, C., and Cox, L.M. (2023). The gut microbiota is an emerging target for improving brain health during ageing. Gut Microbiome (Camb) *4*, E2. https://doi.org/10.1017/gmb.2022.11.
11. Xing, C., Huang, X., Wang, D., Yu, D., Hou, S., Cui, H., and Song, L. (2023). Roles of bile acids signaling in neuromodulation under physiological and pathological conditions. Cell Biosci. *13*, 106. https://doi.org/10.1186/s13578-023-01053-z.
12. Mortiboys, H., Furmston, R., Bronstad, G., Aasly, J., Elliott, C., and Bandmann, O. (2015). UDCA exerts beneficial effect on mitochondrial dysfunction in LRRK2(G2019S) carriers and in vivo. Neurology *85*, 846–852. https://doi.org/10.1212/WNL.0000000000001905.
13. Wu, X., Liu, C., Chen, L., Du, Y.-F., Hu, M., Reed, M.N., Long, Y., Suppiramaniam, V., Hong, H., and Tang, S.-S. (2019). Protective effects of tauroursodeoxycholic acid on lipopolysaccharide-induced cognitive impairment and neurotoxicity in mice. Int. Immunopharmacol. *72*, 166–175. https://doi.org/10.1016/j.intimp.2019.03.065.
14. Zangerolamo, L., Vettorazzi, J.F., Rosa, L.R.O., Carneiro, E.M., and Barbosa, H.C.L. (2021). The bile acid TUDCA and neurodegenerative disorders: An overview. Life Sci. *272*, 119252. https://doi.org/10.1016/j.lfs.2021.119252.
15. Perez, M.-J., and Briz, O. (2009). Bile-acid-induced cell injury and protection. World J. Gastroenterol. *15*, 1677–1689. https://doi.org/10.3748/wjg.15.1677.
16. Xie, G., Wang, X., Jiang, R., Zhao, A., Yan, J., Zheng, X., Huang, F., Liu, X., Panee, J., Rajani, C., et al. (2018). Dysregulated bile acid signaling contributes to the neurological impairment in murine models of acute and chronic liver failure. EBioMedicine *37*, 294–306. https://doi.org/10.1016/j.ebiom.2018.10.030.
17. Carey, M.C., and Small, D.M. (1972). Micelle formation by bile salts. Physical-chemical and thermodynamic considerations. Arch. Intern. Med. *130*, 506–527.
18. Christfort, J.F., Strindberg, S., Plum, J., Hall-Andersen, J., Janfelt, C., Nielsen, L.H., and Müllertz, A. (2019). Developing a predictive in vitro dissolution model based on gastrointestinal fluid characterisation in rats. Eur. J. Pharm. Biopharm. *142*, 307–314. https://doi.org/10.1016/j.ejpb.2019.07.007.
19. Swales, J.D., Papadimitriou, M., and Wrong, O.M. (1973). Observations upon ammonia absorption from the human ileum. Gut *14*, 697–700. https://doi.org/10.1136/gut.14.9.697.
20. Cesca, F., Baldelli, P., Valtorta, F., and Benfenati, F. (2010). The synapsins: key actors of synapse function and plasticity. Prog. Neurobiol. *91*, 313–348. https://doi.org/10.1016/j.pneurobio.2010.04.006.
21. Frommherz, L., Bub, A., Hummel, E., Rist, M.J., Roth, A., Watzl, B., and Kulling, S.E. (2016). Age-Related Changes of Plasma Bile Acid

Concentrations in Healthy Adults–Results from the Cross-Sectional KarMeN Study. PLoS One *11*, e0153959. https://doi.org/10.1371/journal.pone.0153959.

22. Amador-Noguez, D., Dean, A., Huang, W., Setchell, K., Moore, D., and Darlington, G. (2007). Alterations in xenobiotic metabolism in the long-lived Little mice. Aging Cell *6*, 453–470. https://doi.org/10.1111/j.1474-9726.2007.00300.x.

23. Bertolotti, M., Gabbi, C., Anzivino, C., Crestani, M., Mitro, N., Del Puppo, M., Godio, C., De Fabiani, E., Macchioni, D., Carulli, L., et al. (2007). Age-related changes in bile acid synthesis and hepatic nuclear receptor expression. Eur. J. Clin. Invest. *37*, 501–508. https://doi.org/10.1111/j.1365-2362.2007.01808.x.

24. Borkowski, K., Taha, A.Y., Pedersen, T.L., De Jager, P.L., Bennett, D.A., Arnold, M., Kaddurah-Daouk, R., and Newman, J.W. (2021). Serum metabolomic biomarkers of perceptual speed in cognitively normal and mildly impaired subjects with fasting state stratification. Sci. Rep. *11*, 18964. https://doi.org/10.1038/s41598-021-98640-2.

25. Ma, J., Hong, Y., Zheng, N., Xie, G., Lyu, Y., Gu, Y., Xi, C., Chen, L., Wu, G., Li, Y., et al. (2020). Gut microbiota remodeling reverses aging-associated inflammation and dysregulation of systemic bile acid homeostasis in mice sex-specifically. Gut Microb. *11*, 1450–1474. https://doi.org/10.1080/19490976.2020.1763770.

26. Brown, J., Theisler, C., Silberman, S., Magnuson, D., Gottardi-Littell, N., Lee, J.M., Yager, D., Crowley, J., Sambamurti, K., Rahman, M.M., et al. (2004). Differential expression of cholesterol hydroxylases in Alzheimer's disease. J. Biol. Chem. *279*, 34674–34681. https://doi.org/10.1074/jbc.M402324200.

27. Gao, T., Feridooni, H.A., Howlett, S.E., and Pelis, R.M. (2017). Influence of age on intestinal bile acid transport in C57BL/6 mice. Pharmacol. Res. Perspect. *5*, e00287. https://doi.org/10.1002/prp2.287.

28. Lee, G., Lee, H., Hong, J., Lee, S.H., and Jung, B.H. (2016). Quantitative profiling of bile acids in rat bile using ultrahigh-performance liquid chromatography-orbitrap mass spectrometry: Alteration of the bile acid composition with aging. J. Chromatogr. B Analyt. Technol. Biomed. Life Sci. *1031*, 37–49. https://doi.org/10.1016/j.jchromb.2016.07.017.

29. Ycaza Herrera, A., and Mather, M. (2015). Actions and interactions of estradiol and glucocorticoids in cognition and the brain: Implications for aging women. Neurosci. Biobehav. Rev. *55*, 36–52. https://doi.org/10.1016/j.neubiorev.2015.04.005.

30. Leite, G., Pimentel, M., Barlow, G.M., Chang, C., Hosseini, A., Wang, J., Parodi, G., Sedighi, R., Rezaie, A., and Mathur, R. (2021). Age and the aging process significantly alter the small bowel microbiome. Cell Rep. *36*, 109765. https://doi.org/10.1016/j.celrep.2021.109765.

31. Sheng, L., Jena, P.K., Hu, Y., and Wan, Y.-J.Y. (2021). Age-specific microbiota in altering host inflammatory and metabolic signaling as well as metabolome based on the sex. Hepatobiliary Surg. Nutr. *10*, 31–48. https://doi.org/10.21037/hbsn-20-671.

32. Savarino, V., Vigneri, S., and Celle, G. (1999). The 13C urea breath test in the diagnosis of Helicobacter pylori infection. Gut *45* (*Suppl 1*), I18–I22. https://doi.org/10.1136/gut.45.2008.i18.

33. Jo, D., Kim, B.C., Cho, K.A., and Song, J. (2021). The Cerebral Effect of Ammonia in Brain Aging: Blood-Brain Barrier Breakdown, Mitochondrial Dysfunction, and Neuroinflammation. J. Clin. Med. *10*, 2773. https://doi.org/10.3390/jcm10132773.

34. McCue, J.D. (1987). Gram-negative bacillary bacteremia in the elderly: incidence, ecology, etiology, and mortality. J. Am. Geriatr. Soc. *35*, 213–218. https://doi.org/10.1111/j.1532-5415.1987.tb02311.x.

35. Vince, A., Dawson, A.M., Park, N., and O'Grady, F. (1973). Ammonia production by intestinal bacteria. Gut *14*, 171–177. https://doi.org/10.1136/gut.14.3.171.

36. Zhang, L., Li, M., Zhan, L., Lu, X., Liang, L., Su, B., Sui, H., Gao, Z., Li, Y., Liu, Y., et al. (2015). Plasma metabolomic profiling of patients with diabetes-associated cognitive decline. PLoS One *10*, e0126952. https://doi.org/10.1371/journal.pone.0126952.

37. Baloni, P., Funk, C.C., Yan, J., Yurkovich, J.T., Kueider-Paisley, A., Nho, K., Heinken, A., Jia, W., Mahmoudiandehkordi, S., Louie, G., et al. (2020). Metabolic Network Analysis Reveals Altered Bile Acid Synthesis and Metabolism in Alzheimer's Disease. Cell Rep. Med. *1*, 100138. https://doi.org/10.1016/j.xcrm.2020.100138.

38. Zhang, S.-Y., Li, R.J.W., Lim, Y.-M., Batchuluun, B., Liu, H., Waise, T.M.Z., and Lam, T.K.T. (2021). FXR in the dorsal vagal complex is sufficient and necessary for upper small intestinal microbiome-mediated changes of TCDCA to alter insulin action in rats. Gut *70*, 1675–1683. https://doi.org/10.1136/gutjnl-2020-321757.

39. Keitel, V., Görg, B., Bidmon, H.J., Zemtsova, I., Spomer, L., Zilles, K., and Häussinger, D. (2010). The bile acid receptor TGR5 (Gpbar-1) acts as a neurosteroid receptor in brain. Glia *58*, 1794–1805. https://doi.org/10.1002/glia.21049.

40. Massafra, V., Milona, A., Vos, H.R., Ramos, R.J.J., Gerrits, J., Willemsen, E.C.L., Ramos Pittol, J.M., Ijssennagger, N., Houweling, M., Prinsen, H.C.M.T., et al. (2017). Farnesoid X Receptor Activation Promotes Hepatic Amino Acid Catabolism and Ammonium Clearance in Mice. Gastroenterology *152*, 1462–1476.e10. https://doi.org/10.1053/j.gastro.2017.01.014.

41. Wang, H., Tan, Y.-Z., Mu, R.-H., Tang, S.-S., Liu, X., Xing, S.-Y., Long, Y., Yuan, D.-H., and Hong, H. (2021). Takeda G Protein-Coupled Receptor 5 Modulates Depression-like Behaviors via Hippocampal CA3 Pyramidal Neurons Afferent to Dorsolateral Septum. Biol. Psychiatry *89*, 1084–1095. https://doi.org/10.1016/j.biopsych.2020.11.018.

42. Huff, M.W., Telford, D.E., Edwards, J.Y., Burnett, J.R., Barrett, P.H.R., Rapp, S.R., Napawan, N., and Keller, B.T. (2002). Inhibition of the apical sodium-dependent bile acid transporter reduces LDL cholesterol and apoB by enhanced plasma clearance of LDL apoB. Arterioscler. Thromb. Vasc. Biol. *22*, 1884–1891. https://doi.org/10.1161/01.atv.0000035390.87288.26.

43. Xiao, J., Dong, L.-W., Liu, S., Meng, F.-H., Xie, C., Lu, X.-Y., Zhang, W.J., Luo, J., and Song, B.-L. (2023). Bile acids-mediated intracellular cholesterol transport promotes intestinal cholesterol absorption and NPC1L1 recycling. Nat. Commun. *14*, 6469. https://doi.org/10.1038/s41467-023-42179-5.

44. Chen, L., Yao, X., Young, A., McNulty, J., Anderson, D., Liu, Y., Nystrom, C., Croom, D., Ross, S., Collins, J., et al. (2012). Inhibition of apical sodium-dependent bile acid transporter as a novel treatment for diabetes. Am. J. Physiol. Endocrinol. Metab. *302*, E68–E76. https://doi.org/10.1152/ajpendo.00323.2011.

45. Nowell, J., Blunt, E., and Edison, P. (2023). Incretin and insulin signaling as novel therapeutic targets for Alzheimer's and Parkinson's disease. Mol. Psychiatry *28*, 217–229. https://doi.org/10.1038/s41380-022-01792-4.

46. Zhao, G., Zhang, T., Liu, W., Edderkaoui, M., Hu, R., Li, J., Pandol, S.J., Fu, X., and Han, Y.-P. (2022). Sequestration of Intestinal Acidic Toxins by Cationic Resin Attenuates Pancreatic Cancer Progression through Promoting Autophagic Flux for YAP Degradation. Cancers *14*, 1407. https://doi.org/10.3390/cancers14061407.

47. Wispelwey, B., Lesse, A.J., Hansen, E.J., and Scheld, W.M. (1988). Haemophilus influenzae lipopolysaccharide-induced blood brain barrier permeability during experimental meningitis in the rat. J. Clin. Invest. *82*, 1339–1346. https://doi.org/10.1172/JCI113736.

48. Cheng, X., Buckley, D., and Klaassen, C.D. (2007). Regulation of hepatic bile acid transporters Ntcp and Bsep expression. Biochem. Pharmacol. *74*, 1665–1676. https://doi.org/10.1016/j.bcp.2007.08.014.

49. Chen, T., Zhou, K., Sun, T., Sang, C., Jia, W., and Xie, G. (2022). Altered bile acid glycine : taurine ratio in the progression of chronic liver disease. J. Gastroenterol. Hepatol. *37*, 208–215. https://doi.org/10.1111/jgh.15709.

50. Sang, C., Wang, X., Zhou, K., Sun, T., Bian, H., Gao, X., Wang, Y., Zhang, H., Jia, W., Liu, P., et al. (2021). Bile Acid Profiles Are Distinct among

Patients with Different Etiologies of Chronic Liver Disease. J. Proteome Res. *20*, 2340–2351. https://doi.org/10.1021/acs.jproteome.0c00852.

51. Cui, L., Huang, L., Pan, F.-F., Wang, Y., Huang, Q., Guan, Y.-H., Lo, C.-Y.Z., Guo, Y.-H., Chan, A.S., Xie, F., and Guo, Q.H. (2023). Chinese Preclinical Alzheimer's Disease Study (C-PAS): Design and Challenge from PET Acceptance. J. Prev. Alzheimers Dis. *10*, 571–580. https://doi.org/10.14283/jpad.2023.49.

52. Ren, Z., Yu, J., Wu, Z., Si, W., Li, X., Liu, Y., Zhou, J., Deng, R., and Chen, D. (2018). MicroRNA-210-5p Contributes to Cognitive Impairment in Early Vascular Dementia Rat Model Through Targeting Snap25. Front. Mol. Neurosci. *11*, 388. https://doi.org/10.3389/fnmol.2018.00388.

53. Zheng, Z., Wei, J., Hou, X., Jia, F., Zhang, Z., Guo, H., Yuan, F., He, F., Ke, Z., Wang, Y., and Zhao, L. (2022). A High Hepatic Uptake of Conjugated Bile Acids Promotes Colorectal Cancer-Associated Liver Metastasis. Cells *11*, 3810. https://doi.org/10.3390/cells11233810.

54. Haghighat, N., McCandless, D.W., and Geraminegad, P. (2000). The effect of ammonium chloride on metabolism of primary neurons and neuroblastoma cells in vitro. Metab. Brain Dis. *15*, 151–162. https://doi.org/10.1007/BF02679981.

55. Wang, Z., Wang, H., Peng, Y., Chen, F., Zhao, L., Li, X., Qin, J., Li, Q., Wang, B., Pan, B., and Guo, W. (2020). A liquid chromatography-tandem mass spectrometry (LC-MS/MS)-based assay to profile 20 plasma steroids in endocrine disorders. Clin. Chem. Lab. Med. *58*, 1477–1487. https://doi.org/10.1515/cclm-2019-0869.

STAR★METHODS

KEY RESOURCES TABLE

REAGENT or RESOURCE	SOURCE	IDENTIFIER
Antibodies		
Rabbit polyclonal anti-SYN1	Proteintech	Cat#20258-1-AP, RRID: AB_2800493
Mouse monoclonal anti-PSD95	Abcam	Cat#20665-1-AP, RRID: AB_300453
Rabbit monoclonal anti-β-Actin	Cell Signaling Technology	Cat#4970, RRID: AB_2223172
Anti-rabbit, HRP-linked	Cell Signaling Technology	Cat#7074, RRID: AB_2099233
Anti-mouse, HRP-linked	Cell Signaling Technology	Cat#7076, RRID: AB_330924
Anti-rabbit, Alex Flour 488-linked	Abcam	Cat#ab150077, RRID: AB_2630356
Anti-mouse, Alex Flour 647-linked	Abcam	Cat#ab150179, RRID: AB_2884038
Biological samples		
Serum from mice	This paper	N/A
Tissues from mice	This paper	N/A
Chemicals, peptides, and recombinant proteins		
Phosphate buffered saline	Sigma	Cat#P2272, CAS: NA
Paraformaldehyde	Sigma	Cat#158127, CAS: 30525-89-4
RIPA buffer	Beyotime Biotechnology	Cat#P0013C, CAS: NA
DNase I	Sigma	Cat#11284932001, CAS: NA
Papain	Sigma	Cat#232-627-2, CAS: 9001-73-4
B-27	Gibco	Cat#17504044
L-glutamine	Gibco	Cat#25030149
Critical commercial assays		
Asbt Elisa kit (for rat)	Jiangsu Mei Biao Biological Technology Co., Ltd.	Cat#MB-7410A
Asbt Elisa kit (for mouse)	Jiangsu Mei Biao Biological Technology Co., Ltd.	Cat#MB-6453A
Syn1 Elisa kit (for rat)	S.A.B	Cat#EK3880
Syn1 Elisa kit (for mouse)	S.A.B	Cat#EK6728-2
Ammonia Assay Kit	Sigma-Aldrich	Cat#AA0100,
SYBR Green PCR Master Mix	Vazyme	Cat#A25742
Pierce BCA Protein Assay Kit	Thermo Fisher	Cat#23227
Clarity Western ECL Substrate	Bio-Rad	Cat#1705060
Experimental models: Cell lines		
Rat primary hippocampal neurons	This paper	N/A
Experimental models: Organisms/strains		
Wistar rat	Vital River laboratory animal technology Co. Ltd., Beijing, China	N/A
C57BL/6J mouse	Shanghai SLAC Laboratory Animal Co., Ltd	N/A
Software and algorithms		
GraphPad Prism 9.3 software	GraphPad Software	http://www.graphpad.com/
Adobe Illustrator	Adobe	https://www.adobe.com/products/illustrator.html
TargetLynx 4.2	Waters Corporation	N/A
Microsoft 365	Microsoft	https://www.microsoft.com/zh-cn/microsoft-365/buy/compare-all-microsoft-365-products?tab=1

(*Continued on next page*)

Continued

REAGENT or RESOURCE	SOURCE	IDENTIFIER
Other		
PAGE Gel Fast Preparation Kit	EpiZyme	Cat#PG112
PageRuler Prestained Protein Ladder	Thermo Fisher	Cat#26616
Immobilon-PSQ PVDF Membrane	Millipore	Cat#ISEQ00010
Fetal Bovine Serum	Gibco	Cat#10100147C
Penicillin-streptomycin (5000U/mL)	Gibco	Cat#15140122
Neurobasal medium	Gibco	Cat#21103049
DMEM/F12 (1:1)	Invitrogen	Cat#11330-032
Laser-scanning confocal microscope	Zeiss	Zeiss LSM 900, Germany)

RESOURCE AVAILABILITY

Lead contact

Further information and requests for resources and reagents should be directed to and will be fulfilled by the lead contact, Wei Jia (weijia2@hku.hk).

Materials availability

This study did not generate new unique reagents.

Data and code availability

- This paper does not report the original code.
- Any additional information required to reanalyze the data reported in this paper is available from the lead contact upon request.
- The metabolomics data of cohort III is from ADNI, which can be found at www.adni-info.org and www.loni.usc.edu/ADNI/.

EXPERIMENTAL MODEL AND STUDY PARTICIPANT DETAILS

Human study

Cohort I

All the biospecimens of human participants (Total, male female)used in this study were obtained from the Biorepository of Metabolic Diseases at the Shanghai Sixth People's Hospital affiliated to Shanghai Jiao Tong University School of Medicine. The samples from the participants are all the healthy controls in the Biorepository and obtained from multiple cohort studies.[49,50]The inclusion and exclusion criteria are as follows: (1) Age between 20 and 80 years old; (2) No medical history within 2 months; (3) No history of metabolic, cardiovascular, gastrointestinal diseases, stroke, craniocerebral injury, brain tumor, anxiety, depression, or other conditions potentially impacting cognitive function adversely.

Cohort II

Chinese Preclinical Alzheimer's Disease Study (C-PAS).

C-PAS is a nationwide longitudinal study aimed at identifying biomarkers for early detection and progression tracking of Alzheimer's disease (AD). Inclusion and exclusion criteria, clinical and neuroimaging protocols, and other information about C-PAS are described here.[51] The ethics committee of Shanghai Sixth People's Hospital Affiliated to Shanghai Jiao Tong University School of Medicine reviewed and approved this study (2019-032), following the principles of the Declaration of Helsinki. Written informed consent was obtained from participants or their caregivers. All relevant ethical regulations were followed during the study.

Participants in the C-PAS that selected in this study had to fulfill the following criteria: (1) Age between 40 and 89 years with a minimum education duration of more than 1 year; (2) Absence of severe hearing or visual impairment, and proficiency in Mandarin communication; (3) No history of stroke, craniocerebral injury, brain tumor, anxiety, depression, or other conditions potentially impacting cognitive function adversely; (4) The Chinese version of Addenbrooke's Cognitive Examination-III (ACE-III-CV)3 were selected as brief cognitive screening tests.

Cohort of ADNI

Alzhemer's disease neuroimaging initiative (ADNI), launched in 2003, is a longitudinal multi-center study designed to develop clinical, imaging, genetic, and biochemical biomarkers for the early detection and tracking of AD. Inclusion and exclusion criteria, clinical and neuroimaging protocols, and other information about ADNI can be found at www.adni-info.org. Demographic information, apolipoprotein E (APOE-4) ε4 genotype, neuropsychological test scores, and clinical information were downloaded from the ADNI data repository (www.loni.usc.edu/ADNI/). Written informed consent was obtained at the time of enrollment, which included permission for analysis and data sharing. The consent forms used were approved by each participating sites' institutional review board.

Rats and mice experiments

All animal studies were approved by the Institutional Animal Care and Use Committee at the Center for Laboratory Animals, Shanghai Sixth People's Hospital Affiliated to Shanghai Jiao Tong University School of Medicine (Shanghai, China). All the rats and mice were maintained in a specific-pathogen-free (SPF) environment in controlled conditions with free access to food and water (12 h light/dark cycle at 20°C–22°C, humidity 45% ± 5%). Rats and mice were acclimated in an animal facility with chow diet and *ad libitum* for one week. The chow diet (TP23522, Trophic Animal Feed High-tech Co., Ltd, China) was used in animal experiments. During the experiments, the body weights and food intake were measured once a week.

Aging animal modeling

Wistar rats and C57BL6J mice (8 weeks) were randomly grouped based on the two time points of sacrifice at 24 weeks (24w, $n = 8$ per gender) and 111 weeks (111w, $n = 6$ per gender). After behavioral performance was acquired, rodents were anesthetized, and serum, brain, ileum, ileal contents and colon contents were immediately collected and stored at −80°C for future use.

Chemical manipulation of ASBT in rats and mice

Wistar rats and C57BL6J mice (3-month old) were randomly divided into four groups (n = 12/group; 6 per gender) respectively, and those in Control (treated with the same value of Normal saline), DEX (Dexamethasone,1 mg/kg), DEX+GSK (Dexamethasone, 1 mg/kg; GSK2330672, 1 mg/kg) groups were intragastrically administrated with drugs for two weeks respectively. Rats' behavioral performance was acquired. Rodents were anesthetized, and serum, brain, ileum, ileal contents were immediately collected and stored at −80°C for future use.

METHOD DETAILS

Cognitive performance tests

The open-field test (OFT) was used to analyze spontaneous exploratory activity and evaluate rats' or mice's cognizing levels. The OFT was performed under bright interior lighting, and the open-field apparatus included an appropriate size floor and high walls (the chamber for rat 100 × 100 × 40 cm and for mice 45 × 45 × 40 cm, RWD Science Co., Shenzhen, China). The bed was divided into nine squares with black lines, including the central and boundary areas. Each rat or mouse was gently placed in the central region and adapted to the environment for 2 min; then rat or mouse separately was left free to explore the open field for 5 min. The room was kept quiet during the test, and the apparatus was cleaned with 75% ethanol after each trial. The time spent, including cumulative durations and the central area's movement distance, was recorded. The data were analyzed using a video camera and processed with the corresponding software.

The Y-maze was used to measure working memory by exploring areas that have not been previously explored. The Y maze apparatus with three plexiglass branches (for rats 50 cm long, 16 cm wide, and 32 cm high, for mice 30 cm long, 8 cm wide, and 15 cm high, RWD Science Co., Shenzhen, China) was elevated above the floor. During the 10 min test, rats were placed at the bottom arm (A1) facing the center, and they could choose between the left arm (A2) and the right arm (A3). Entry into an arm was defined as placement of the four paws into the arm, and spontaneous alteration was defined as a triplet of consecutive entries to different branches. Animals that did not reach the criteria, including a minimum of 5 entries and 2 min without a new movement or entry, were excluded. The room was kept quiet during the test, and the apparatus was cleaned with 75% ethanol after each trial. The percentage of alternations was calculated as the number of actual alternations divided by the maximum number of alternations (the total number of arm entries minus 2). The data were analyzed using a video camera and processed with the corresponding software.

Transmission electron microscope

Brain tissues were fixed with 2.5% glutaraldehyde in cacodylate buffer (0.1 M, pH 7.4) for 1 h at 4°C, incubated in Tris–HCl (0.05 M, pH 9.0) containing diaminobenzidine (2.5 mg/mL) and H_2O_2(10 mL/mL of a 3% solution) for 1 h at 21°C, washed in cacodylate buffer (0.1 M, pH 7.4) for 5 min at 21°C, post-fixed in 1% (w/v) osmium tetroxide that was diluted in cacodylate sodium solution (0.1 M, pH 7.4) for 1 h at 21°C in the dark, and rinsed in cacodylate buffer (0.1 M, pH7.4). All incubations were processed in the absence of light. The preparations were then dehydrated in graded ethanol solutions and embedded. Ultrathin sections were cut with an ultramicrotome, contrasted with uranyl acetate and lead citrate, and were examined with a Transmission Electron Microscope (TEM) (JEOL 2100F, Japan).

Primary neuronal culture and intervention

Primary hippocampal neurons were isolated and cultured as previously reported.[52] The pregnant rat at E17–E19 days of gestation was sacrificed, and the pups were taken out, and then their heads were cut off. The brain was exposed, and the hippocampus was isolated and washed with pre-cooled phosphate-buffered saline (PBS) and moved into a 6 mL DMEM/F12 medium (Invitrogen) that contained papain (2 mg/mL, Sigma) and DNase I (0.1 mg/mL, Sigma)for digestion in a 37°C incubator for 20 min with a gentle shake every 5 min. The collections were centrifuged at 1,000 rpm for 8 min and then suspended in the culture medium containing 10% FBS. We calculated the viable cell rate to 92% using trypan blue staining. As recommendation, 7×10^5 viable cells were plated into 35 mm Bottom Petri Dish (∅ = 20 mm, Nest). After 2 days of culture in complete culture medium(Neurobasal medium containing 1/50 diluted

B-27 and 1/100 diluted L-glutamine), neurons were then treatmented with TCA (25 and 50 μM, refers to evidence[53]) and ammonia (2.5 and 5 mM, refers to evidence[54]) for 24 h, followed by mRNA or protein were harvested for analysis.

ELISA assays

The Syn1 or ASBT protein was extracted from the hippocampal tissue or distal intestine and determined using a Syn1(for rat: EK3880, for mouse: EK6728–2, S.A.B) or ASBT (for mouse: MB-6453A, for rat: MB-7410A, Jiangsu Mei Biao Biological Technology Co., Ltd.) assay kit according to the manufacturer's instruction.

LC-MS/MS-based quantification of bile acids

According to previously reported methods, BAs in serum, intestine, intestinal contents, and brain were measured.[55] Briefly, for BAs analysis, the sample extract was mixed with 150 μL of methanol containing internal standards (IS, 0.10 μM of CA-D4, DCA-D4, GCA-D4, and LCA-D4) and then incubated for 10 min in room temperature. After centrifugation at 20,000 g for 10 min, the supernatant was transferred to a clean tube, vacuum dried, and reconstituted with 40 μL acetonitrile (with 0.1% formic acid) and 40 μL water (with 0.1% formic acid). After centrifugation, the supernatant was used for LC-MS/MS analysis.

Chromatographic separations of BAs were performed using an ACQUITY BEH C8 column (1.7 μm, 100 mm × 2.1mminternal dimensions, Waters, Milford, MA) or an ACQUITY BEH C18 column (1.7 μm, 100 mm × 2.1mminternal dimensions, Waters, Milford, MA). A waters ACQUITY ultra-performance LC system coupled with a waters XEVO TQ-S mass spectrometer with an ESI source controlled by MassLynx4.1 software (Waters, Milford, MA) was used for all analyses. UPLC-MS raw data were obtained with positive and negative modes. TargetLynx applications manager version 4.1 (Waters Corp., Milford, MA) was used to obtain calibration equations and the quantitative concentration of each bile acid in the samples.

Ammonia measurements

The serum and hippocampus of rats and mice were acquired, and the ammonia levels were measured using an Ammonia Assay Kit (AA0100, Sigma-Aldrich) according to the manufacturer's protocols.

Quantitative PCR determination

According to the manufacturer's protocol, total RNA was isolated from liver, brain, and intestinal tissue using TRIzol reagent (15596026, Life technologies, USA) and Direct-zol RNA MinPrep Plus (R2072, Zymo). The concentration of total RNA was measured using a Nanodrop 2000 (Thermo Fisher Scientific, Waltham, MA, USA) spectrometer. The primers of qPCR analysis were synthesized by Sangon Biotech (Shanghai, China). The quantitative real-time PCR reaction was conducted with Power Up SYBR Green PCR Master Mix (A25742, Applied Biosystems, USA). The reaction was accomplished by QuantStudio 7 Flex Real-Time System (Applied Biosystems Instruments, USA). Gapdh was used as a housekeeping gene, and the relative expression of the target genes was calculated using the comparative Ct approach (dCT). The sequences are listed as follows in Table S1.

Western blot

Brain tissue lysates from the hippocampal tissues were obtained, and protein concentrations were tested using a BCA protein assay kit (23227#, Thermo, California, CA). Equal amounts of protein samples were separated by SDS-PAGE and transferred to 0.22μm PVDF membranes, which were then blocked at room temperature for 1h in 5% BSA TBST solutions. Membranes were incubated with the primary antibodies Syn1(1:5,000, ab254349, Abcam), Psd95 (1:5,000; ab13552, Abcam), and β-Actin (1:1000, 4970S, CST) overnight at 4°C, followed by a 1h incubation at room temperature with HRP-conjugated goat anti-rabbit secondary antibody (1:3,000, 7074S, CST) or HRP-conjugated Horse anti-mouse secondary antibody (1:3,000, 7074S, CST). The bands were then obtained and analyzed with the MP90 (Bio-Rad). β-Actin served as an internal control, and experiments were repeated 3 times.

Immunofluorescence staining

Cells were fixed with PFA for 30 min at room temperature, permeabilized with 0.1% Triton X-100/PBS for 10min, and then incubated with primary antibody for Syn1 (1:250; 20258-AP, Proteintech) and Psd95 (1:250; ab13552, Abcam) overnight at 4°C. The cells were washed 3 times using PBS on the second day and incubated with the secondary antibodies, Alexa Flour 488 (1:1,000; ab150077, Abcam) or Alexa Flour 647 (1:1,000; ab150179, Abcam) for 2 h at room tempreture, followed by washed 3 times using PBS. After incubated with DAPI for 10 min at room temperature and washing 3 times by PBS, the samples were ready for observation.

Synapse analysis

The samples were examined using a confocal microscope (LSM880, Zeiss). The green puncta indicate the staining of Syn1, marking the presynaptic membrane, while the red puncta represent the Psd95 staining, highlighting the postsynaptic membrane. The merged staining of Syn1 and Psd95 represents a complete synapse and the zoomed details indicated by the white arrow. For each sample, three randomly acquired fields of view were assessed, and colocalized puncta were counted. The ratio of the density of the merged staining of Syn1 and Psd95 to the DAPI-labeled cell number was presented.

QUANTIFICATION AND STATISTICAL ANALYSIS

The statistics were performed using GraphPad Prism 9.3 (GraphPad Software, CA, USA). The differences in comparison of genes, proteins, and metabolites among rodent groups in both genders were analyzed with two-way ANOVA; and those in cultured neurons and Cholestyramine treated mice were analyzed with One-way ANOVA; Pearson r correlation analysis was applied to analyze the relationship between BAs, ammonia, cognitive score, and Syn1. *, $p < 0.05$; **, $p < 0.01$; ***, $p < 0.001$.